Published in final edited form as:
Hear Res. 2014 April ; 310: 69–75. doi:10.1016/j.heares.2014.01.008.

Auditory Responses to Electric and Infrared Neural Stimulation of the Rat Cochlear Nucleus

Rohit Verma[1,3], **Amelie A. Guex**[4], **Kenneth E. Hancock**[3], **Nedim Durakovic**[3], **Colette M. McKay**[2,5], **Michaël C. C. Slama**[3,6], **M. Christian Brown**[3,6], and **Daniel J. Lee**[3,6]

[1]School of Medicine, University of Manchester, UK [2]School of Psychological Sciences, University of Manchester, UK [3]Eaton-Peabody Laboratories, Massachusetts Eye and Ear Infirmary, Switzerland [4]Ecole Polytechnique Fédérale de Lausanne, Switzerland [5]The Bionics Institute of Australia, Melbourne, Australia [6]Department of Otology and Laryngology, Harvard Medical School, Boston, MA 02114, USA

Abstract

In an effort to improve the auditory brainstem implant, a prosthesis in which user outcomes are modest, we applied electric and infrared neural stimulation (INS) to the cochlear nucleus in a rat animal model. Electric stimulation evoked regions of neural activation in the inferior colliculus and short-latency, multipeaked auditory brainstem responses (ABRs). Pulsed INS, delivered to the surface of the cochlear nucleus via an optical fiber, evoked broad neural activation in the inferior colliculus. Strongest responses were recorded when the fiber was placed at lateral positions on the cochlear nucleus, close to the temporal bone. INS-evoked ABRs were multipeaked but longer in latency than those for electric stimulation; they resembled the responses to acoustic stimulation. After deafening, responses to electric stimulation persisted, whereas those to INS disappeared, consistent with a reported “optophonic” effect, a laser-induced acoustic artifact. Thus, for deaf individuals who use the auditory brainstem implant, INS alone did not appear promising as a new approach.

Keywords

Auditory brainstem implant; prosthesis; laser; optical stimulation

1. Introduction

The auditory brainstem implant (ABI) is the primary rehabilitative option for deaf patients who cannot receive the cochlear implant due to damage of the auditory nerve (from a tumor, surgery or trauma), scarring of the cochleae, or severe inner ear dysplasia. In the ABI, a surface electrode array bypasses the auditory nerve and electrically stimulates the cochlear nucleus (CN). Unlike most cochlear implant users, the majority of ABI users do not achieve

Corresponding author: M. Christian Brown, Eaton-Peabody Laboratory, Massachusetts Eye and Ear Infirmary, 243 Charles St., Boston, MA, USA. Phone: 617-573-3875. Fax: 617-720-4408. Chris_Brown@meei.harvard.edu.

Preliminary versions of this work were presented at the 2012 meeting of the Association for Research in Otolaryngology and are contained in a master’s thesis (Guex, 2012).

open set word recognition (Colletti et al., 2012; Otto et al., 1998). A number of theories have been proposed to explain these differences, including damage to the CN from tumor growth or surgery to remove a tumor, limited access to the tonotopic organization of the CN with surface stimulation, suboptimal placement of the electrode array, and poor spatial specificity associated with electric current spread (Colletti and Shannon, 2005; Otto et al., 1998; Shannon et al., 1993). Consistent with the latter two ideas, ABI users often experience side effects from stimulation of non-auditory pathways, resulting in facial nerve symptoms, dizziness, throat and tongue sensations and limb pain (Shannon et al., 1993). Electrodes with such side effects must be turned off when the ABI processor is programmed.

Infrared neural stimulation (INS) is a technique in which pulsed infrared radiation produced by a laser is used to stimulate neural tissue. This technique has been applied to the sciatic nerve (Wells et al., 2007b), cavernous nerves (Fried et al., 2008), facial nerve (Teudt et al., 2007), vestibular nerve (Harris et al., 2009), and the cochlea (Izzo et al., 2006; Izzo et al., 2007; Richter et al., 2008). The INS method may be more spatially selective than electric stimulation. For example, INS applied to different portions of the sciatic nerve evokes contraction in different muscle groups (Wells et al., 2007a), presumably because it only stimulates the part of the nerve within the optical beam path. In the auditory system, INS applied to the cochlea evokes midbrain responses with spatial tuning curves that can be as narrow as those evoked by acoustic tones (Richter et al., 2011). However, INS has not been previously applied to the CN, and whether it evokes responses in a broad or narrow pattern is not known.

In this study, using a rat model, we applied INS to the CN. The response metrics used were the auditory brainstem response (ABR) and neural responses in the inferior colliculus (IC). The ABR neural generators, at least to acoustic stimuli, are specific populations of auditory neurons in the ventral subdivision of the CN, the superior olivary complex, and inferior colliculus that respond with temporal synchrony (Melcher and Kiang, 1996). The neural responses from the IC, by contrast, are less dependent on synchrony and likely reflect the inputs from both the dorsal and ventral CN subdivisions (Oliver, 1984; Schofield, 2001) as well as inputs from the superior olivary complex (Glendenning et al., 1992; Schofield, 2002). To compare to INS responses, we also evoked responses to electric stimulation, which is the method of exciting neurons used by the ABI. An electrically evoked response (eABR) consists of several waveform peaks (Abbas and Brown, 1988; Abbas and Brown, 1991; Nevison, 2006; O'Driscoll et al., 2011; van den Honert and Stypulkowski, 1986; Waring, 1995; Waring et al., 1999), but has shorter latency than its acoustically evoked counterpart. Electric stimulation of the CN also evokes strong neural responses in the IC (Hoa et al., 2008; McCreery et al., 1998; Shivdasani et al., 2008). By using both hearing and deafened preparations, we studied which portions of these responses were due to the "optophonic" phenomenon associated with the use of a pulsed infrared radiant laser source (Teudt et al., 2011). Our overall conclusions are that, used alone, INS does not seem to offer a clear avenue toward improving the ABI.

2. Materials and Methods

2.1 Anesthesia and Surgery

All procedures were conducted in accordance with guidelines of the NIH and were approved by the Animal Care and Use Committee of the Massachusetts Eye and Ear Infirmary and Harvard Medical School. Experiments were conducted within a sound-attenuating chamber. Data were obtained from 30 adult male Sprague-Dawley rats (370–600 g). Anesthesia was ketamine (800 mg/kg i.p.) and xylazine (8 mg/kg i.p.). Atropine (0.4 mg/kg) was given to minimize respiratory secretions. Dexamethasone (0.8 mg/kg) was administered at induction to minimize brain swelling during surgery. Booster injections of ketamine (30 mg/kg i.p.)

and/or xylazine (3 mg/kg i.p.) were given every hour as required after paw pinch assessment.

A tracheal cannula was placed, and the rat was positioned on a warming pad and positioned on an animal platform in a stereotactic head holder with bars that stabilized the head placed rostral to the ear canals (David Kopf Instruments, Tujunga, CA). A posterior craniectomy was created and the dura overlying the left cerebellum was exposed. The dura was incised with a cruciate incision and surface blood vessels on the cerebellum thermo-cauterized. The left half of the cerebellum was gently aspirated to successively reveal the left CN and associated brainstem at the caudal end of the fourth ventricle. The exposed brainstem surface was kept moist by the application of 0.9% NaCl and covered with gelfoam. A separate mini-craniotomy was performed over the right temporo-parietal suture, rostral to the tentorium. After incision of the dura, this craniotomy provided access to the IC. A closed-field sound system was placed in the left ear canal. In 6 animals, after pre-deafening data were collected, a cut was made of the left auditory nerve at the central edge of the internal auditory meatus to deafen the animal on that side.

2.2 Electric and Infrared Neural Stimulation

Electric current pulses were delivered to the surface of the left CN using a pair of stainless steel wires insulated except at the tip (200 μm diam.; impedance 0.1–0.5 MΩ). Bipolar, biphasic pulses (100 μs duration) were presented through a stimulus isolator (Model 2200, A-M Systems, Carlsborg, WA) at 27 pulses/s. Infrared pulses for INS were generated using a diode laser (Capella R-1850, Lockheed-Martin Aculight Corp., Bothell, WA). The laser unit was kept outside the sound-attenuating chamber and the optical fiber (400 μm diam.) was led into the chamber via a penetration hole. The distal fiber was mounted to a three-axis micromanipulator and its tip was placed on the surface of the left CN. Unless explicitly stated otherwise, laser parameters were: pulse duration of 0.25 ms, stimulation rate of 23 Hz, and wavelength of 1849 nm. This wavelength is expected to penetrate into the tissue about 700 μm (Hale and Querry, 1973). Radiant energy of the laser was measured with a high-sensitivity thermopile sensor (PS19Q, Coherent, Santa Clara, CA).

2.3 IC Recordings

Multi-unit recordings were made with a 16 channel penetrating electrode array (A1×16-5mm-150–177, Neuronexus, Ann Arbor, MI), with a global reference. The array was inserted into the central part of the right IC through the overlying occipital cortex using a 3-D micromanipulator (David Kopf Instruments Tujunga, CA) bolted to the headholder. Signals were high-pass filtered with a forward and reverse Butterworth filter of order 5 with a 500 Hz cutoff frequency, and sampled with 16-bit resolution at 20 kHz. Electrode insertion was in a dorsal to ventral trajectory along the tonotopic axis of the IC. Correct placement was confirmed by neural responses recorded across the full length of the array during acoustic stimulation to the left ear using tone pips (20 ms duration; 1 – 32 kHz in increments of 2 steps per octave).

For the IC recordings, analysis of the raw data was performed with programs written with Matlab Software. Spikes were detected when the signal exceeded a threshold defined as four times the median of the signal containing spontaneous activity. Spontaneous activity was measured in each recording as the spike count with no stimulation. The time window for counting spikes was the interval from 5 – 25 ms after stimulus onset. The number of spikes was averaged over 32 trials. Activation was defined as the mean spike count across all electrodes for each stimulation level.

2.4 ABR Recordings

ABRs were recorded between needle electrodes placed sub-cutaneously at the vertex and the left (ipsilateral) ear, with a ground electrode placed on the back. The signal was filtered with an analog bandpass filter (30 Hz – 3 kHz), amplified by 60 dB (Ithaco Model 1201, DL Instruments, Ithaca NY), A/D converted (sampling at 25 kHz) and averaged (acoustic: 512 avgs; electric: 100 avgs; INS: 512 avgs). The first millisecond of electrically generated ABR signals, containing the stimulus artifact, was ignored. The INS-generated ABRs were digitally filtered with a forward and reverse band-pass Butterworth filter of order 5, with cut-off frequencies of 200 and 2.5 kHz. The RMS of the first 10 ms of the ABR waveform was calculated with Matlab Software (The Mathworks Inc., Natick, MA.).

2.5 Acoustic Measurements

Acoustic recordings of the optophonic effect produced by the laser were performed with a Larson-Davis 1/8 inch condenser microphone placed 1 mm from the tip of the optical fiber and in contraposition to it.

2.6 Reconstruction of the CN

To investigate which subdivision of the CN was stimulated, a 3D model of the cochlear nucleus (Guex, 2012) was constructed using a reconstruction software package (AMIRA, Mercury Computer Systems, Berlin, Germany, Version 5.4.2). For this purpose, serial sections (40 μm thickness) of a right Nissl-stained brainstem of a rat were imaged with a compound microscope and loaded into the software. Successive images were then aligned manually. The subdivisions were identified according to the histological criteria in the rat (Paxinos and Watson, 1998) and the guinea pig (Hackney et al., 1990). The reconstruction was “mirror-imaged” to be comparable to the left side CN used for the experiments.

3. Results

3.1 Responses to acoustic stimulation in hearing animals

Acoustic stimulation with tone bursts evoked IC neural responses that were tonotopically organized (Fig. 1). In the example illustrated, the response to 1.0 kHz appeared only on the electrodes with high numbers (12–16). These high-numbered electrodes are located dorsally in the IC (numbers are arranged according to depth, Fig. 1B, inset). Responses to successively higher frequencies were present on successively lower-number electrodes, ending with the response to 32 kHz on electrode numbers 2–6 (located ventrally). The response areas were narrow, with each acoustic frequency represented, at least for low sound levels, on a relatively small number of electrodes. At each electrode, the frequency causing a response at the lowest sound level was defined as the characteristic frequency. The mapping of characteristic frequency vs. electrode number is shown in Figure 1B. The range of 2–32 kHz characteristic frequencies were represented for this particular preparation. Such tonotopic mappings were found in all 19 rats examined.

Acoustic stimulation with clicks produced the example ABR waveform seen in Fig. 2A, which had a large positive peak at a latency about 2 ms and smaller earlier and later peaks.

3.2 Responses to electric stimulation

Electric stimulation of the CN also produced robust responses in the IC (Figs. 3, 4). With electric stimulation, the parameter of sound frequency was no longer available, so we varied the location of stimulation across the surface of the CN as the parameter (Fig. 3B, C). This stimulated portion of the CN is almost certainly the dorsal subdivision (DCN), because, as seen in a 3-D reconstruction (Fig. 3C), the DCN is the superficial and visible subdivision.

Locations at ventrolateral positions of the DCN receive input from auditory nerve fibers of low characteristic frequencies and more dorsomedial sites receive input from higher characteristic frequencies (Fig. 3C, arrow; Muniak et al., 2013; Spirou et al., 1993). This innervation predicts that lateral stimulation locations would activate IC electrodes with high numbers, whereas medial locations would activate electrodes with low numbers. Such a pattern was observed in a broad sense – for example along row B in Figure 3, the response sites in IC moved from middle electrode numbers at stimulation location B1 (lateral) to low electrode numbers at location B4 (medial). At some stimulus locations, areas of IC activation were narrow (A1–A3), but at other locations the areas were broad (B2, B3, C2, C3). Broad activation is also seen in another case (Fig. 4A). This case also shows (along row B) the trend for more lateral-to-medial stimulation progressions evoking response areas that progress from higher-to-lower electrode numbers. This trend held for the overall data set (Fig. 4B), although the spread of data points from the best-fit line indicates variability (Fig. 4B). In the rostro-caudal dimension, there were no systematic changes observed.

Electrically evoked ABRs were multi-peaked (Figs. 2B, 4C). The earliest peaks were obscured by the artifact, but their latency was clearly shorter than the ABRs evoked by acoustic stimulation. Those sites with several waveform peaks at short latencies (< 3 ms), such as Fig. 4C, sites B1–B4 and C2–C4, were those sites that elicited the largest IC responses (Fig. 4A). Our data are not sufficient in extent to know whether there was a regional dependence on ABR waveform. Large, late potentials (Fig. 4C, C4) may represent myogenic responses to spread of stimulation beyond the CN (O'Driscoll et al., 2011; van den Honert and Stypulkowski, 1986).

3.3 Responses to INS

Infrared neural stimulation evoked IC neural responses that were also broad in extent (Fig. 5A). As laser radiant energy was increased, there was a clear threshold, followed increasing firing rates and then saturation of firing. All stimulation locations evoked broad response patterns in the IC, with less variability than that observed for electric stimulation. The INS responses were largest when the optical fiber was positioned at the lateral aspect of the CN (locations A1, B1, and C1) and smaller at more medial positions towards the fourth ventricle. However, the region of IC response did not change in a systematic way with the position of CN stimulation. The INS-evoked ABRs were also largest for lateral stimulation positions (Fig. 5B). Additionally, both IC responses and ABRs were elicited when the optical fiber was aimed at the temporal bone adjacent to the CN. The waveform of the ABR in response to INS was similar to that of acoustic stimulation, with a large positive peak at a latency of about 2 ms and smaller earlier and later peaks (Figs. 2C, 5B). Peak-to-peak ABR amplitude was an increasing function of INS radiant energy up to the limits of our laser (700 mJ/cm^2, data not shown). It decreased slightly as pulse rate varied from 3 to 63 Hz, and was almost unchanged as wavelength was varied across the wavelengths provided by the laser (1849 – 1865 nm).

3.4 Responses in deafened animals

The responses to INS were greatly reduced by deafening the preparation. Figure 6 illustrates exemplary responses before and after section of the auditory nerve in one animal (Fig. 6A, B). Any remaining response was very small and may have resulted from an incomplete section. Section was confirmed to be near-complete by the greater than 60 dB shift in the sound-evoked ABR threshold. In contrast, however, the electrically evoked ABR (Fig. 6C) persisted or even increased in amplitude after nerve section. This observation indicated that the section had not damaged the CN. The average data for all the deafening experiments are shown in Figure 6D for the IC neural responses and in Figure 6E for ABR responses.

Loss of INS responses post-deafening suggests that these responses were actually to an optophonic artifact associated with the delivery of infrared radiant energy via an optical fiber (Teudt et al., 2011). This phenomenon was documented by recording the acoustic signal 1 mm from the tip of the optical fiber while the laser was activated. The sound level produced was an increasing function of laser radiant energy, and came to a plateau at around 60 dB SPL (Fig. 7A). That this sound could evoke responses was confirmed by placing the optical fiber within the ear canal of a normal-hearing subject. This stimulus evoked ABRs that, like the acoustic level of the optophonic sound, increased with increasing radiant energy from the laser (Fig. 7B).

4. Discussion

These studies demonstrate that stimulation of the CN by electric current generates large ABR responses and neural responses in the IC. Although INS applied to the CN also generates responses in hearing preparations, they disappear or are greatly reduced upon deafening. This result, combined with the measurement of an optophonic effect when the laser is activated, strongly suggest that most or all of the INS responses are to an acoustic artifact generated by the laser.

4.1 Responses to electric stimulation

Electric stimulation applied to the surface of the CN evoked robust ABRs, as previously reported in experimental animals (Rosahl et al., 2001) and in humans who are undergoing surgery to receive the auditory brainstem implant (Frohne et al., 2000; O'Driscoll et al., 2011; Waring et al., 1999; Waring, 1998). In our study, the stimulation site was likely to be the dorsal subdivision of the CN, because it is visible and accessible on the dorsal surface of the brainstem (Fig. 3B, C). However, because of possible spread of stimulation current, we are not certain whether the underlying ventral CN subdivisions were also activated. The ABR waveforms were multi-peaked and bear some resemblance to those evoked by acoustic stimulation. However, they are shorter in latency because they result from direct excitation of the CN without the delays caused by acoustic travel, traveling wave in the cochlea, hair cell excitation, hair cell/nerve terminal synapse, and conduction of impulses along the auditory nerve.

CN stimulation at different positions demonstrated an influence on location of maximal response in the IC (Figs 3, 4). Lateral stimulation positions in CN caused more activation in IC electrodes located dorsally (high electrode numbers), whereas medial CN stimulation positions caused more activation in IC recordings located ventrally (low electrode numbers). This pattern follows the mapping of low to high characteristic frequencies in CN (Muniak et al., 2013; Spirou et al., 1993) and in the IC (Richter et al., 2011; Ryan et al., 1982; Snyder et al., 2004). Some of the response patterns to electric stimulation were broader than those for acoustic stimulation (Fig. 2), which may reflect current spread along the tonotopic axis of the CN. Broad tuning has previously been seen with penetrating electrodes positioned in anterolateral regions of the VCN (Shivdasani et al., 2008); the present study's data are not extensive enough to determine the regional dependence from surface stimulation of the DCN. Broad areas of activation demonstrate the challenges of conveying frequency-specific information in neural prostheses such as the ABI.

4.2 Responses to INS

Data from Figure 6 suggests that the CN responses to INS are almost eliminated after deafening. This result is supported by the location studies (Fig. 5), which show strongest INS responses from stimulation positions near the temporal bone. Also, the similarity of waveforms of INS-generated ABRs and acoustically evoked ABRs (Fig. 1) suggest that they

are both generated by a hearing mechanism that stimulates the AVCN or PVCN (Melcher and Kiang, 1996), rather than INS where the stimulation was applied to the DCN (Fig. 3B, C). Presumably, differences in response result from differences in the spectrum of the artifact generated by the laser vs. the acoustic click. The spectrum of the optophonic effect is likely to be broad because it is a brief transient (Teudt et al., 2011), which is consistent with our finding of broad activation of most of the IC (Fig. 5A). The effects of deafening on INS responses are large both for the ABR, which requires temporal synchrony, and for the IC neural responses, where synchrony may be less important for a response. In the auditory periphery, similar effects of deafening were found in one study (Schultz et al., 2012), but other studies (Richter et al., 2008; Richter et al., 2011) found responses persist even in deaf animals and over the same energy levels (26–711 mJ/cm^2 vs. 0–957 mJ/cm^2 in. Peripherally, the response may be mediated by spiral ganglion cells, which may have membrane channels that are responsive to thermal effects of INS (Wells et al., 2007b). Also, INS may provide better stimulation of diverse types of nerve (Fried et al., 2008; Teudt et al., 2007; Wells et al., 2007b) compared to nuclei like the CN. Our data suggest that the central branches of the auditory nerve, which persist after section in our CN preparation, cannot mediate a significant response to INS.

Teudt et al (Teudt et al., 2011) demonstrated that the lasers used for INS can generate an acoustic artifact of up to 60 dB SPL, and we confirm this finding in the present study. We have demonstrated that at radiant energy levels required to generate ‘optical’ brainstem responses, there is an acoustic artifact sufficiently large to stimulate the peripheral auditory system. The large effect of deafening on optically evoked responses of the auditory system would appear to suggest that the mechanism underlying our results is in fact primarily the optophonic effect of the laser. Other optogenetic methods for neural stimulation are available (Boyden et al., 2005) and they appear to offer more suitable alternatives to infrared stimulation of the cochlear nucleus (Darrow et al., 2013; Shimano et al., 2012). They could form the basis for the next-generation ABI.

Acknowledgments

Supported by the Helene and Grant Wilson Auditory Brainstem Implant Program at the Massachusetts Eye and Ear Infirmary, a Med-EL Hearing Solutions Research Grant, the Bertarelli Foundation, and the Paul and Daisy Soros Fellowship for New Americans. The Bionics Institute acknowledges the support it receives from the Victorian Government through its Operational Infrastructure Support Program. We thank Lockheed-Martin for supplying the Aculite laser, and Ishmael Stefanov, Evan Foss, and Haobing Wang for technical assistance.

Abbreviations

ABI	auditory brainstem implant
ABR	auditory brainstem response
AN	auditory nerve
AVCN	anteroventral subdivision of the cochlear nucleus
CN	cochlear nucleus
CF	characteristic frequency
DCN	dorsal subdivision of the cochlear nucleus
eABR	electrically evoked auditory brainstem response
IC	inferior colliculus
INS	infrared neural stimulation

PVCN	posteroventral subdivision of the cochlear nucleus
SPL	sound pressure level
VN	vestibular nerve

References

Abbas PJ, Brown CJ. Electrically evoked brainstem potentials in cochlear implant patients with multielectrode stimulation. Hear Res. 1988; 36:153–162. [PubMed: 3209488]

Abbas PJ, Brown CJ. Electrically evoked auditory brainstem response: Growth of response with current level. Hearing Res. 1991; 51:123–138.

Boyden ES, Zhang F, Bamberg E, Nagel G, Deisseroth K. Millisecond-timescale, genetically targeted optical control of neural activity. Nat Neurosci. 2005; 8:1263–1268. [PubMed: 16116447]

Colletti L, Shannon RV, Colletti V. Auditory brainstem implants for neurofibromatosis type 2. Curr Opin Otolaryngol Head Neck Surg. 2012; 20:353–357. [PubMed: 22886036]

Colletti V, Shannon RV. Open set speech perception with auditory brainstem implant? Laryngoscope. 2005; 115:1974–1978. [PubMed: 16319608]

Darrow KN, Slama M, Kempfle J, Boyden E, Polley D, Brown MC, Lee DJ. Optogenetic control of central auditory neurons. Assoc Res Otolaryngol Abstr. 2013; #695

Fried NM, Lagoda GA, Scott NJ, Su LM, Burnett AL. Noncontact stimulation of the cavernous nerves in the rat prostate using a tunable-wavelength thulium fiber laser. J Endocrinol/Endourological Society. 2008; 22:409–413.

Frohne C, Matthies C, Lesinski-Schiedat A, Battmer RD, Samii M, Lenarz T. Extensive monitoring during auditory brainstem implant surgery. J Laryngol Otol. 2000; 114:11–14.

Glendenning KK, Baker BN, Hutson KA, Masterton RB. Acoustic chiasm V: Inhibition and excitation in the ipsilateral and contralateral projections of LSO. J Comp Neurol. 1992; 319:100–122. [PubMed: 1317390]

Guex, A. Characterization of the auditory system responses to infrared neural stimulation of the cochlear nucleus. School of Life Sciences. Master project in Bioengineering, Ecole Polytechnique Federale de Lausanne; Lausanne, Switzerland: 2012.

Hackney CM, Osen KK, Kolston J. Anatomy of the cochlear nuclear complex of the guinea pig. Anat Embryol. 1990; 182:123–149. [PubMed: 2244686]

Hale GM, Querry MR. Optical constants of water in the 200 nm to 200 μm region. Appl Opt. 1973; 12:555–563. [PubMed: 20125343]

Harris DM, Bierer SM, Wells JD, Phillips JO. Optical nerve stimulation for a vesibular prosthesis. Proc SPIE. 2009; 7180:71800R.

Hoa M, Guan Z, Auner G, Zhang J. Tonotopic responses in the inferior colliculus following electrical stimulation of the dorsal cochlear nucleus of guinea pigs. Otolaryngol Head Neck Surg. 2008; 139:152–155. [PubMed: 18585579]

Izzo AD, Richter CP, Jansen ED, Walsh JT Jr. Laser stimulation of the auditory nerve. Lasers in Surg Med. 2006; 38:745–753. [PubMed: 16871623]

Izzo AD, Walsh JT Jr, Jansen ED, Bendett M, Webb J, Ralph H, Richter CP. Optical parameter variability in laser nerve stimulation: A study of pulse duration, repetition rate, and wavelength. IEEE Trans Biomed Eng. 2007; 54:1108–1114. [PubMed: 17554829]

McCreery DB, Shannon RV, Moore JK, Chatterjee M. Accessing the tonotopic organization of the ventral cochlear nucleus by intranuclear microstimulation. IEEE Trans Rehabil Eng. 1998; 6:391–399. [PubMed: 9865886]

Melcher JR, Kiang NYS. Generators of the brainstem auditory evoked potential in cat III: Identified cell populations. Hearing Res. 1996; 93:52–71.

Muniak MA, Rivas A, Montey KL, May BJ, Francis HW, Ryugo DK. 3D model of frequency representation in the cochlear nucleus of the CBA/J mouse. J Comp Neurol. 2013; 521:1510–1532. [PubMed: 23047723]

Nevison B. A guide to the positioning of brainstem implants using intraoperative electrical auditory brainstem responses. Adv Otorhinolaryngol Basel, Karger. 2006; 64:154–166.

O'Driscoll M, El-Deredy W, Atas A, Sennaroglu G, Sennaroglu L, Ramsden RT. Brain stem responses evoked by stimulation with an auditory brain stem implant in children with cochlear nerve aplasia or hypoplasia. Ear Hear. 2011; 32:300–312. [PubMed: 21150625]

Oliver DL. Dorsal cochlear nucleus projections to the inferior colliculus in the cat: A light and electron microscopic study. J Comp Neurol. 1984; 224:155–172. [PubMed: 19180810]

Otto SR, Shannon RV, Brackmann DE, Hitselberger WE, Staller S, Menapace C. The multichannel auditory brain stem implant: Performance in twenty patients. Otolaryngol - Head & Neck Surgery. 1998; 118:291–303.

Paxinos, G.; Watson, C. The Rat Brain in Stereotaxic Coordinates. Academic Press; San Diego: 1998.

Richter CP, Bayon R, Izzo AD, Otting M, Suh E, Goyal S, Hotaling J, Walsh JT Jr. Optical stimulation of auditory neurons: Effects of acute and chronic deafening. Hearing Res. 2008; 242:42–51.

Richter CP, Rajguru SM, Matic AI, Moreno EL, Fishman AJ, Robinson AM, Suh E, Walsh JT Jr. Spread of cochlear excitation during stimulation with pulsed infrared radiation: inferior colliculus measurements. J Neural Eng. 2011; 8:0560006.

Rosahl SK, Mark G, Herzog M, Pantazis C, Gharabaghi F, Matthies C, Brinker T, Samii M. Far-field responses to stimulation of the cochlear nucleus by microsurgically placed penetrating and surface electrodes in the cat. J Neurosurg. 2001; 95:845–852. [PubMed: 11702876]

Ryan AF, Woolf NK, Sharp FR. Tonotopic organization in the central auditory pathway of the mongolian gerbil: a 2-deoxyglucose study. J Comp Neurol. 1982:207. [PubMed: 7076893]

Schofield BR. Origins of projections from the inferior colliculus to the cochlear nucleus in guinea pigs. J Comp Neurol. 2001; 429:206–220. [PubMed: 11116215]

Schofield BR. Ascending and descending projections from the superior olivary complex in guinea pigs: Different cells project to the cochlear nucleus and the inferior colliculus. J Comp Neurol. 2002; 453:217–225. [PubMed: 12378584]

Schultz M, Baumhoff P, Maier H, Teudt IU, Kruger A, Lenarz T, Kral A. Nanosecond laser pulse stimulation of the inner ear - a wavelength study. Biomed Opt Express. 2012; 3:3332–3345. [PubMed: 23243582]

Shannon RV, Fayad J, Moore J, Lo WW, Otto S, Nelson RA, O'Leary M. Auditory brainstem implant: II. Postsurgical issues and performance. Otolaryngol Head Neck Surg. 1993; 108:634–642. [PubMed: 8516000]

Shimano T, Fyk-Kolodziej B, Asako M, Tomoda K, Bledsoe SC, Pan ZH, Molitor S, Holt AG. Assessment of the AAV-mediated expression of channelrhopdopsin-2 and halorhodopsin in brainstem neurons mediating auditory signaling. Brain Res. 2012; 1511:138–152. [PubMed: 23088961]

Shivdasani MN, Mauger SJ, Rathbone GD, Paolini AG. Inferior colliculus responses to multichannel microstimulation of the ventral cochlear nucleus: Implications for auditory brain stem implants. J Neurophsysiol. 2008; 99:1–13.

Snyder RI, Bierer JA, Middlebrooks JC. Topographic spread of inferior colliculus activation in response to acoustic and intracochlear electric stimulation. J Assoc Res Otolaryngol. 2004; 5:305–322. [PubMed: 15492888]

Spirou GA, May BJ, Wright DD, Ryugo DK. Frequency organization of the dorsal cochlear nucleus in cats. J Comp Neurol. 1993; 329:36–52. [PubMed: 8454725]

Teudt IU, Nevel A, Izzo AD, Walsh JT Jr, Richter CP. Optical stimulation of the facial nerve: a new monitoring technique? Laryngoscope. 2007; 117:1641–1647. [PubMed: 17607145]

Teudt IU, Maier H, Richter CP, Kral A. Acoustic events and "optophonic" cochlear responses induced by pulsed near-infrared laser. IEEE Trans Biomed Eng. 2011; 58:1648–1655. [PubMed: 21278011]

van den Honert C, Stypulkowski PH. Characterization of the electrically evoked auditory brainstem response (ABR) in cats and humans. Hearing Res. 1986; 21:109–126.

Waring M. Intraoperative electrophysiologic monitoring to assist placement of auditory brain stem implant. Ann Otol Rhinol Laryngol. 1995; 103 (166):33–36.

Waring M, Ponton C, Don M. Activating separate ascending auditory pathways produces different human thalamic/cortical responses. Hearing Res. 1999; 130:219–229.

Waring MD. Refractory properties of auditory brainstem responses evoked by electrical stimulation of human cochlear nucleus; evidence of neural generators. Electroenceph Clin Neurophysiol. 1998; 108:331–344. [PubMed: 9714375]

Wells J, Kao C, Konrad P, Mahadevanen-Jansen M, Jansen ED. Pulsed laser versus electrical energy for peripheral nerve stimulation. J Neurosci Meth. 2007a; 163:326–337.

Wells J, Kao C, Konrad P, Milner T, Kim J, Mahadevanen-Jansen M, Jansen ED. Biophysical mechanisms of transient optical stimulation of peripheral nerve. Biophys J. 2007b; 93:2567–2580. [PubMed: 17526565]

Highlights

- Electric and infrared neural stimulation (INS) was applied to the cochlear nucleus.
- Electric stimulation elicited collicular and auditory brainstem responses (ABRs).
- INS also elicited colliculular responses & ABRs similar to acoustically-evoked ABRs.
- Deafening decreased INS responses, suggesting their generation by a laser artifact.

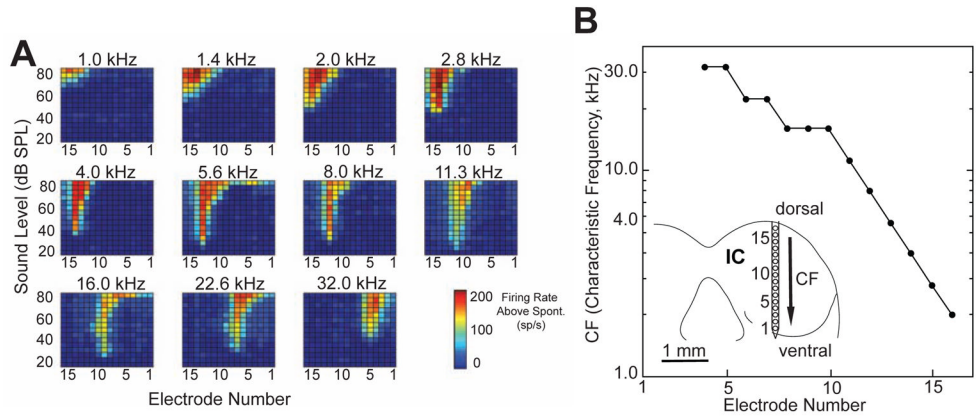

Figure 1.

Neural activity recorded in the IC in response to acoustic stimulation. A) Response areas for individual pure tones presented to the contralateral ear. Each panel is a plot of the firing rate at each of the 16 electrodes as a function of sound level. Color indicates firing rate above spontaneous activity (see scale). B) Graph of characteristic frequency (CF) as a function of electrode number within the IC. Higher characteristic frequencies were found ventrally (deeper within the IC), whereas lower characteristic frequencies were found dorsally (more superficial). Inset schematizes a tangential view of the IC, the multi-channel recording electrode and its electrode numbers, and the tonotopic progression of CFs (arrow).

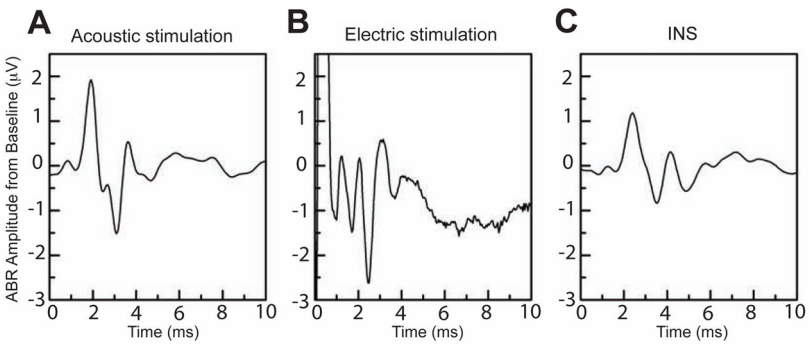

Figure 2.

Example ABR waveforms from acoustic stimulation, electric stimulation and INS. A) Acoustic click, 40 dB SPL; average of 512 presentations. B) Electric stimulation: current,0.4 mA; 100 μs duration; 27 pulses/s; average of 100 presentations. C) INS: radiant energy, 711 mJ/cm^2; 0.25 ms duration; rate, 23 Hz; wavelength, 1849 nm; average of 512 presentations.

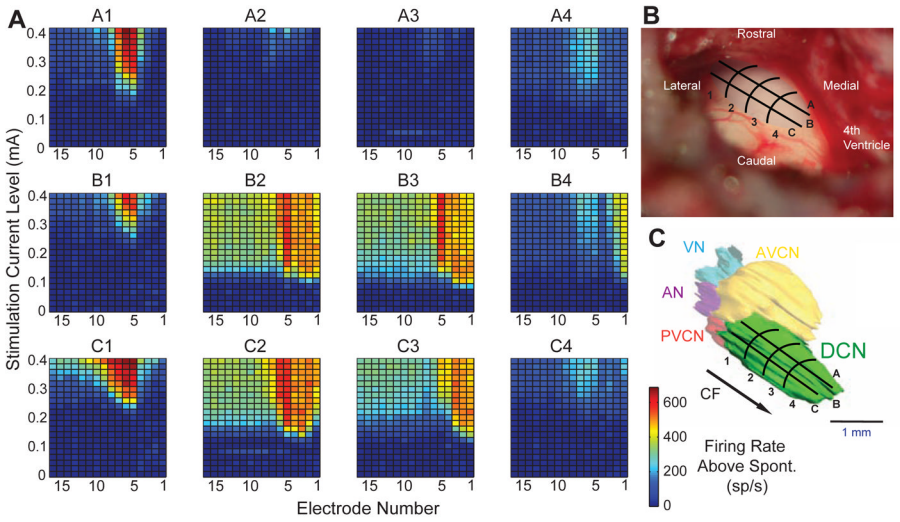

Figure 3.

A) Neural responses in the IC to electric stimulation of the contralateral CN. Each panel is a plot of the firing rate at each of the 16 electrodes as a function of stimulation current. Each response area is from stimulation of a different CN location, with the locations indicated above each graph. Locations appear on a grid superimposed on a photomicrograph of a surface view of the CN (B) and on a 3-D reconstruction (C). The grid's anatomical reference point at site C4 was the caudal end of the 4th ventricle. The reconstruction also indicates that the exposed surface is mostly the dorsal subdivision (DCN), whereas other subdivisions are deeper in the brain (as indicated by the opaque shading). Arrow shows the approximate axis of the DCN's tonotopic progression of CFs found in other studies (Muniak et al., 2013; Spirou et al., 1993). AVCN: anteroventral subdivision of the CN; PVCN: posteroventral subdivision of the CN; AN: auditory nerve stump; VN: vestibular nerve stump.

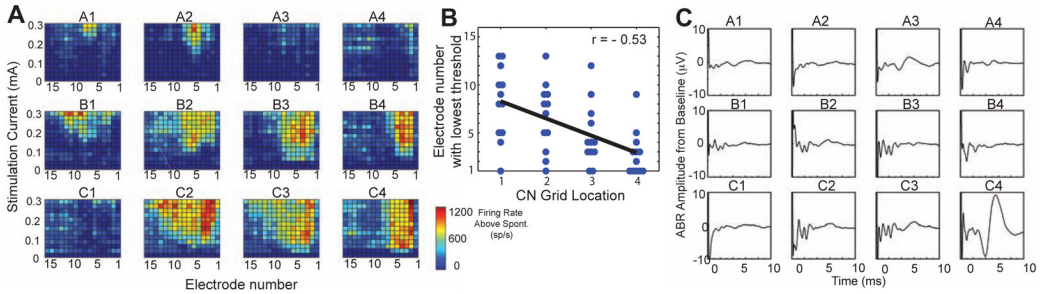

Figure 4.

Responses to electric stimulation in a second case. A) IC neural response areas from stimulation of the CN at different locations using the previous grid (Figs. 3B, C). B) Plot of electrode with the lowest threshold as a function of CN grid location (averaged across the lettered rows) for all data of the present study. Line shows best linear regression fit to the data. C) Electrically-evoked ABRs at the same CN locations as in A. The large deviation of the trace in the initial portion is the stimulus artifact. Electric stimulus: 0.4 mA.

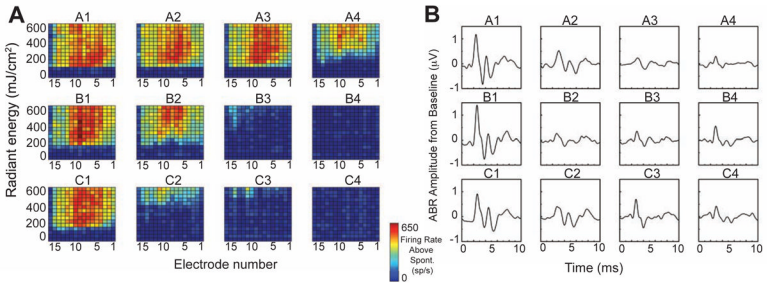

Figure 5.

Responses to INS. A) IC response areas from stimulation of the CN at different locations using the grid (Figs. 3B, C). B) ABR waveforms at the same locations as in A. INS stimuli: 711 mJ/cm^2 for ABRs.

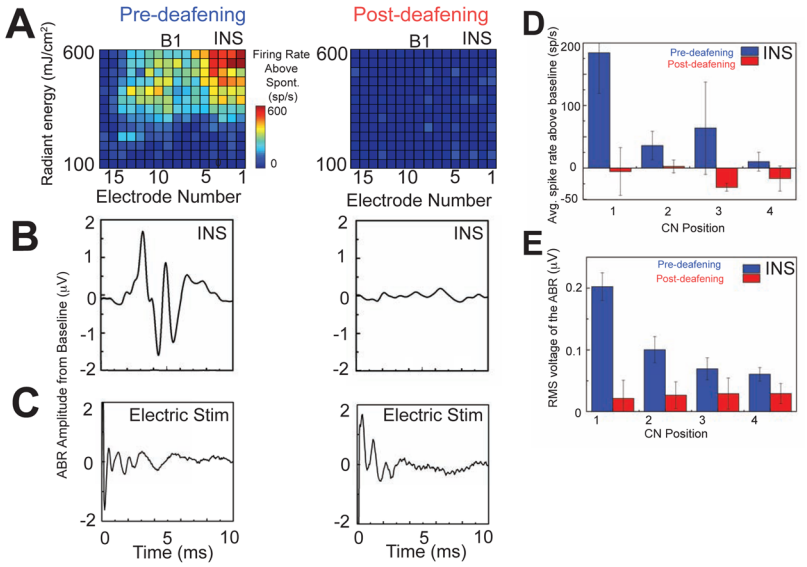

Figure 6.

Large effect of deafening on INS, but not electric, responses. INS-evoked neural response area (A) and ABRs (B) from stimulation at location B1 before and after deafening. INS stimuli: 711 mJ/cm^2 radiant energy for ABRs. C) Electrically-evoked ABR before and after deafening. Electric stimulus: 0.2 mA. D) Summary of IC neural responses to INS, pre- and post-deafening. Average spike rates are across five experiments (bars show standard errors). E) Summary of the ABR responses to INS effects, pre- and post-deafening. Average RMS of the waveforms from six experiments (bars show standard errors).

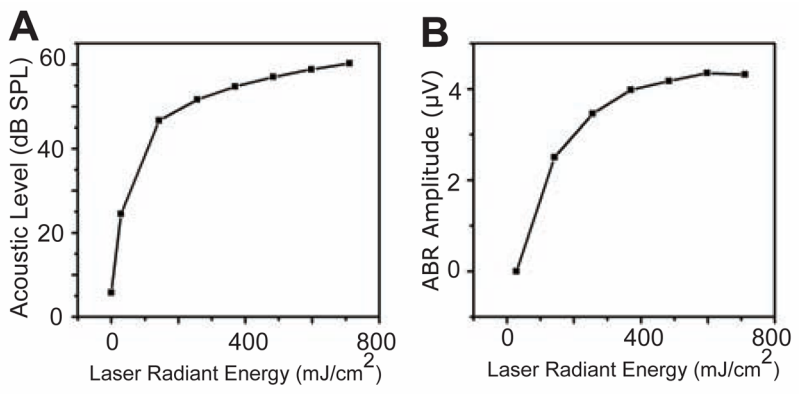

Figure 7.

A) Measurement of the noise generated by the optical fiber tip at increasing radiant energies. B) Amplitude of ABR (peak-to-peak measurement) generated by placing the optical fiber in the ear canal in a single experiment.